DFTT 14/94
April 1994

Heavy Quark Production at e^+e^- Colliders in Multijet Events and a New Method of Computing Helicity Amplitudes[1]

Alessandro Ballestrero, Ezio Maina and Stefano Moretti

Dipartimento di Fisica Teorica, Università di Torino
and INFN, Sezione di Torino
v. Giuria 1, 10125 Torino, Italy.

Abstract

Heavy quark production in multijet events at e^+e^- colliders is studied at tree level. Total production rates are given and compared with the corresponding results for massless quarks. A new method of computing helicity amplitudes is briefly sketched.

[1] Talk presented at the XXIXth Rencontres de Moriond, QCD and High Energy Hadronic Interactions, Méribel - Savoie - France March 19–26, 1994.

e–mail: ballestrero,maina,moretti@to.infn.it

Introduction

The great number of hadronic decays of the Z^0 observed at LEP provides the opportunity to test our understanding of strong interactions in unprecedented detail. Large samples of multi–jet events have been accumulated and analyzed [1, 2]. Recent advances in b–tagging techniques based on the introduction of vertex detectors and on a refinement of the selection procedures, with their large efficiencies and the resulting high purities, have paved the way to the study of heavy–quark production in association with light–quark and gluon jets.

It has been pointed out in series of papers [3, 4, 5] that the effects of the b–quark mass are substantial and increase with the number of jets. We have studied jet production at tree level taking full account of γ, Z interference and of quark masses. These latter reduce the available phase space and strongly decrease the emission of gluons collinear with the quark direction, the so called "dead cone effect". In particular we have computed:

- $e^+e^- \to Q\bar{Q}g$
- $e^+e^- \to Q\bar{Q}gg$
- $e^+e^- \to Q_1\bar{Q}_1Q_2\bar{Q}_2$
- $e^+e^- \to Q\bar{Q}\gamma$
- $e^+e^- \to Q\bar{Q}\gamma g$
- $e^+e^- \to Q\bar{Q}\gamma\gamma$
- $e^+e^- \to Q\bar{Q}ggg$
- $e^+e^- \to Q_1\bar{Q}_1Q_2\bar{Q}_2g$

We have used $M_Z = 91.1$ GeV, $\Gamma_Z = 2.5$ GeV, $\sin^2(\theta_W) = .23$, $m_b = 5.$ GeV, $\alpha_{em} = 1/128$ and $\alpha_s = .115$ in the numerical part of our work.

When the number of Feynman diagrams becomes large it is convenient to compute the amplitudes using helicity methods instead of computing directly the amplitude squared. We have used two of the most popular formalism [6, 7] in our calculations. Both methods can be easily implemented in a small set of nested subroutines. This however results in computer programs which are too slow. For the five–jet case we have resorted to the symbolic package *Mathematica* [8] to write down the Fortran expression for each helicity amplitude. With this procedure we have produced a rather large piece of code, which however runs quite fast, and therefeore can be used in high statistics Montecarlo runs. As an example the program for $q\bar{q}ggg$ production is about 24,000 lines long, but requires only about 5×10^{-2} seconds to evaluate on a Vaxstation 4000/90. This is still acceptable but clearly indicates that faster methods are needed, as the one we have recently developed and used for computing $e^+e^- \to b\bar{b}W^+W^-$ [9, 10].

A new method for helicity amplitude calculations

There are normally three possible ways of evaluating a spinor line. The first consists in reducing the expression to a trace [11]. The second amounts to writing explicitely, for example in the helicity representation [6], the components of the spinors, of the vertex matrices $\not{\eta}_i$'s and of the $\not{p}_i$ and then proceed to the multiplication of the matrices and spinors. The other way [12, 7] consists in decomposing every $\not{p}_i$ in sums of external momenta $\not{k}_i$ and use the relation $\not{k} = \sum_\lambda U(k,\lambda)\overline{U}(k,\lambda) + M$ (with $M = +m$ if $U = u$, $M = -m$ if $U = v$) in order to reduce everything to the computation of expressions of the type $\overline{U}(k_i,\lambda_i)\not{\eta}U(k_j,\lambda_j)$.

We get a remarkable simplification with respect to the procedures sketched above inserting just before every $(\not{p}_i + \mu_i)$ in a spinor line, completeness relations formed with eigenvectors of $\not{p}_i$. To do this we must construct spinors $U(p,\lambda)$ which are defined also for p spacelike. With this method, in addition to reducing ourselves to the computation of expressions of the type $\overline{U}(p_i,\lambda_i)\not{\eta}_i U(p_j,\lambda_j)$, we avoid the proliferation of terms due to the decomposition of the $\not{p}_i$ in terms of external momenta.

One can easily costruct an example of spinors defined for any value of p^2 and satisfying Dirac equation and completeness relation, with a straightforward generalization of those introduced in ref.[7]. One first defines spinors $w(k_0,\lambda)$ for an auxiliary massless vector k_0 satisfying

$$w(k_0,\lambda)\bar{w}(k_0,\lambda) = \frac{1+\lambda\gamma_5}{2}\not{k}_0 \tag{1}$$

and with their relative phase fixed by

$$w(k_0,\lambda) = \lambda\not{k}_1 w(k_0,-\lambda), \tag{2}$$

with k_1 a second auxiliary vector such that $k_1^2 = -1$, $k_0\cdot k_1 = 0$. Spinors for a four momentum p, with $m^2 = p^2$ are then obtained as:

$$u(p,\lambda) = \frac{\not{p}+m}{\sqrt{2\,p\cdot k_0}}\, w(k_0,-\lambda) \qquad v(p,\lambda) = \frac{\not{p}-m}{\sqrt{2\,p\cdot k_0}}\, w(k_0,-\lambda) \tag{3}$$

$$\bar{u}(p,\lambda) = \bar{w}(k_0,-\lambda)\, \frac{\not{p}+m}{\sqrt{2\,p\cdot k_0}} \qquad \bar{v}(p,\lambda) = \bar{w}(k_0,-\lambda)\, \frac{\not{p}-m}{\sqrt{2\,p\cdot k_0}} \tag{4}$$

If p is spacelike, one of the two determination of $\sqrt{p^2}$ has to be chosen for m in the above formulae, but physical results will not depend on this choice.

One can readily check that with the previous definitions, Dirac equations

$$\not{p}u(p) = +mu(p) \qquad \not{p}v(p) = -mv(p) \tag{5}$$

$$\bar{u}(p)\not{p} = +m\bar{u}(p) \qquad \bar{v}(p)\not{p} = -m\bar{v}(p) \tag{6}$$

and the completeness relation

$$1 = \sum_\lambda \frac{u(p,\lambda)\bar{u}(p,\lambda) - v(p,\lambda)\bar{v}(p,\lambda)}{2m} \tag{7}$$

are satisfied also when $p^2 \le 0$ and m is imaginary.

Let us now consider the case in which there are only two insertions in a spinor line:

$$T^{(2)}(p_1;\eta_1;p_2;\eta_2;p_3) = \overline{U}(p_1,\lambda_1)\not{\eta}_1(\not{p}_2+\mu_2)\not{\eta}_2 U(p_3,\lambda_3). \tag{8}$$

One can insert in eq. (8), on the left of $(\not{p}_2+\mu_2)$ the relation (7) and make use of Dirac equations to get:

$$\begin{aligned} T^{(2)} \;=\; & \frac{1}{2}\overline{U}(p_1,\lambda_1)\not{\eta}_1 u(p_2,\lambda_2) \times \bar{u}(p_2,\lambda_2)\not{\eta}_2 U(p_3,\lambda_3) \times \left(1+\frac{\mu_2}{m_2}\right) + \\ & \frac{1}{2}\overline{U}(p_1,\lambda_1)\not{\eta}_1 v(p_2,\lambda_2) \times \bar{v}(p_2,\lambda_2)\not{\eta}_2 U(p_3,\lambda_3) \times \left(1-\frac{\mu_2}{m_2}\right) \end{aligned} \tag{9}$$

This example can be generalized to any number of insertions and shows that the factors $(\not{p}_i+\mu_i)$ can be eliminated, reducing all fermion lines essentially to products of T functions:

$$T_{\lambda_1\lambda_2}(p_1;\eta;p_2) = \overline{U}(p_1,\lambda_1)\not{\eta}U(p_2,\lambda_2) \tag{10}$$

defined for any value of p_1^2 and p_2^2.

The T functions (10) have a simple dependence on m_1 and m_2:

$$\widetilde{T}_{\lambda_1\lambda_2}(p_1;\eta;p_2) \equiv \sqrt{p_1\cdot k_0}\,\sqrt{p_2\cdot k_0}\,T_{\lambda_1\lambda_2}(p_1;\eta;p_2) = \tag{11}$$

$$A_{\lambda_1\lambda_2}(p_1;\eta;p_2) + M_1 B_{\lambda_1\lambda_2}(p_1;\eta;p_2) + M_2 C_{\lambda_1\lambda_2}(p_1;\eta;p_2) + M_1 M_2 D_{\lambda_1\lambda_2}(p_1;\eta;p_2)$$

where

$$M_i = +m_i \;\text{ if }\; U(p_i,\lambda_i) = u(p_i,\lambda_i) \qquad M_i = -m_i \;\text{ if }\; U(p_i,\lambda_i) = v(p_i,\lambda_i). \tag{12}$$

The functions A, B, C, D are independent of m_1 and m_2 and of the u or v nature of $\overline{U}(p_1,\lambda_1)$ and $U(p_2,\lambda_2)$. Every $T^{(n)}$, for any number of insertions turns out to be of the form (10) and this greatly simplyfies the rules for evaluating spinor lines [9].

Results

A selection of our results is shown in fig.1 through 3, and we refer to the original papers for more details. In fig.1b we present the cross sections for $e^+e^- \to q\bar{q}g$ and $e^+e^- \to q\bar{q}gg$ with $q = d, b$ as a function of $y_{\rm cut}$ for both the JADE [13] and DURHAM [14] definitions of y at LEP I. The ratio of massive to masslees cross section is shown in fig.1a. For small $y_{\rm cut}^D$ the cross section for $b\bar{b}g$ is almost 20% smaller than for $d\bar{d}g$. As expected the ratio becomes closer to one for larger $y_{\rm cut}$, but for $y_{\rm cut}$ as large as .2, still $R_3^{bd} = \sigma(b\bar{b}g)/\sigma(d\bar{d}g) \leq .96$ in both schemes.

Jet–shape variables have been extensively studied as a tool to determine α_s and as a testing ground for the agreement between data and the standard description of strong interactions. In the ranges used for measuring α_s, the ratio of massive to massless tree–level predictions can significantly differ from unity and it depends both from the variable and from its actual value. We have compared at $O(\alpha_s)$ the ratio $R_{\gamma Z}$, which is obtained from the full matrix element, with R_γ, the ratio which results neglecting the Z^0 (as in JETSET), for Thrust, Oblateness, C-parameter, M_H and M_D. The difference between $R_{\gamma Z}$ and R_γ turns out to be about 1.2×10^{-2}, almost independent of the particular variable and of its specific value. As an example, in fig.2 we show both $R_{\gamma Z}$ and R_γ for the M_H, M_D, C and O distributions.

In fig.3 we show the ratios $\sigma(2b3g)/\sigma(2d3g)$ (continuous line), $\sigma(2u2bg)/\sigma(2u2dg)$ (dashed line) and $\sigma(2d2bg)/\sigma(2d2sg)$ (dotted line) in the two recombination schemes as a function of y_{cut}. These curves confirm our previous conclusions that mass effects increase with the number of final state light partons. The ratio for the dominant $2q3g$ production process is equal to .58 at $y_{cut} = .001$ in the DURHAM scheme and to .67 at $y_{cut} = .005$ in the JADE scheme. It is even smaller for the processes with four quark jets in the final state. This corresponds to a $6\div8\%$ decrease in the predictions for the total five–jet cross section.

When our results for jet production are compared with the data it is to be remebered that we have used $\alpha_s = .115$ which corresponds to $Q^2 = M_{z^0}^2$ with $\Lambda_{\overline{MS}} = 200$ MeV with five active

flavours. The analysis of shape variables and jet rates to $\mathcal{O}(\alpha_s^2)$ has shown that, in order to get agreement between the data and the theoretical predictions, a rather small scale for the strong coupling constant has to be chosen [2].

The flavour independence of the strong coupling constant has been investigated by several groups [15] using both jet–rates and shape variables. Mass corrections have played an important rôle in this study. We look forward to more detailed analyses of QCD in the heavy quark sector.

References

[1] L3 Collaboration, B. Adeva *et al.*, Z. Phys. **C 55** (1992) 39.
ALEPH Collaboration, D. Buskulic *et al.*, Z. Phys. **C 55** (1992) 209.

[2] DELPHI Collaboration, P. Abreu *et al.*, Z. Phys. **C 54** (1992) 55.
OPAL Collaboration, P.D. Acton *et al.*, Z. Phys. **C 55** (1992) 1.

[3] A. Ballestrero, E. Maina and S. Moretti, Phys. Lett. **B294** (1992) 425.

[4] A. Ballestrero, E. Maina and S. Moretti, Torino Preprint DFTT 53-92, October 1992. To appear in Nucl. Phys. B.

[5] A. Ballestrero and E. Maina, Phys. Lett. **B323** (1994) 53.

[6] K. Hagiwara and D. Zeppenfeld, *Nucl. Phys.* **B274** (1986) 1.

[7] F.A. Berends, P.H. Daverveldt and R. Kleiss *Nucl. Phys.* **B253** (1985) 441, R. Kleiss and W.J. Stirling, *Nucl. Phys.* **B262** (1985) 235.
C. Mana and M. Martinez, Nucl. Phys. **B287** (1987) 601.

[8] *Mathematica* is a registered trademark of Wolfram Research, Inc.

[9] A. Ballestrero and E. Maina, Torino Preprint DFTT 76-93, January 1994.

[10] A. Ballestrero, E. Maina and S. Moretti, Torino Preprint DFTT 78-93, March 1994.

[11] M. Caffo and E. Remiddi, *Helv. Phys. Acta.* **55** (1982) 339.
G. Passarino, *Phys. Rev.* **D28** (1983) 2867, *Nucl. Phys.* **B237** (1984) 249.

[12] P. De Causmaecker, R. Gastmans, W. Troosts and T. T. Wu, *Phys. Lett.* **B105** (1981) 215, *Nucl. Phys.* **B206** (1982) 53; F.A. Berends, R. Kleiss,P. De Causmaecker, R. Gastmans, W. Troosts and T. T. Wu, *Nucl. Phys.* **B206** (1982) 61, **B239** (1984) 382, **B239** (1984) 395, **B264** (1986) 243, **B264** (1986) 265.

[13] JADE Collaboration, W. Bartel *et al.*, Z. Phys. **C 33** (1986) 23.
JADE Collaboration, S. Bethke *et al.*, Phys. Lett. **B213** (1988) 235.

[14] N. Brown and W.J. Stirling, Phys. Lett. **B252** (1990) 657; Z. Phys. **C 53** (1992) 629.

[15] L3 Collaboration, B. Adeva *et al.*, Phys. Lett. **B271** (1991) 461.
DELPHI Collaboration, P. Abreu *et al.*, Phys. Lett. **B307** (1993) 221.
OPAL Collaboration, R. Akers *et al.*, Preprint CERN-PPE/93-118, July 1993.

Figure Captions

Fig. 1 In the upper part we show $R_3^{cu} = \sigma(c\bar{c}g)/\sigma(u\bar{u}g)$, $R_3^{bd} = \sigma(b\bar{b}g)/\sigma(d\bar{d}g)$ and $R_4^{bd} = \sigma(b\bar{b}gg)/\sigma(d\bar{d}gg)$ as a function of $y_{\rm cut}$ for y^J (dashed) and y^D (continuous). In the lower part we present the cross sections for $e^+e^- \to b\bar{b}g$ (continuous), $e^+e^- \to d\bar{d}g$ (dashed), $e^+e^- \to b\bar{b}gg$ (chain-dotted) and $e^+e^- \to d\bar{d}gg$ (dotted) as a function of $y_{\rm cut}$ for both definitions of y at $\sqrt{s} = 91.1$ GeV.

Fig. 2 The ratios $R = d\sigma(b\bar{b}g)/d\hat{M}/d\sigma(d\bar{d}g)/d\hat{M}$ for $\hat{M} = M_H/\sqrt{s}$ and $\hat{M} = M_D/\sqrt{s}$ (lower part) and for $\hat{M} = C-parameter$ and $\hat{M} = Oblateness$ (upper part) from the full matrix element (continuous) and from the photon contribution alone (dashed) at $\sqrt{s} = 91.1$ GeV.

Fig. 3 Ratio of massive to massless cross sections for $\sigma(2b3g)/\sigma(2d3g)$ (continuous line), $\sigma(2u2bg)/\sigma(2u2dg)$ (dashed line) and $\sigma(2d2bg)/\sigma(2d2sg)$ (dotted line) in the JADE and DURHAM recombination schemes as a function of y_{cut} at $\sqrt{s} = 91.1$ GeV.

This figure "fig1-1.png" is available in "png" format from:

http://arXiv.org/ps/hep-ph/9405384v1

This figure "fig1-2.png" is available in "png" format from:

http://arXiv.org/ps/hep-ph/9405384v1

This figure "fig1-3.png" is available in "png" format from:

http://arXiv.org/ps/hep-ph/9405384v1

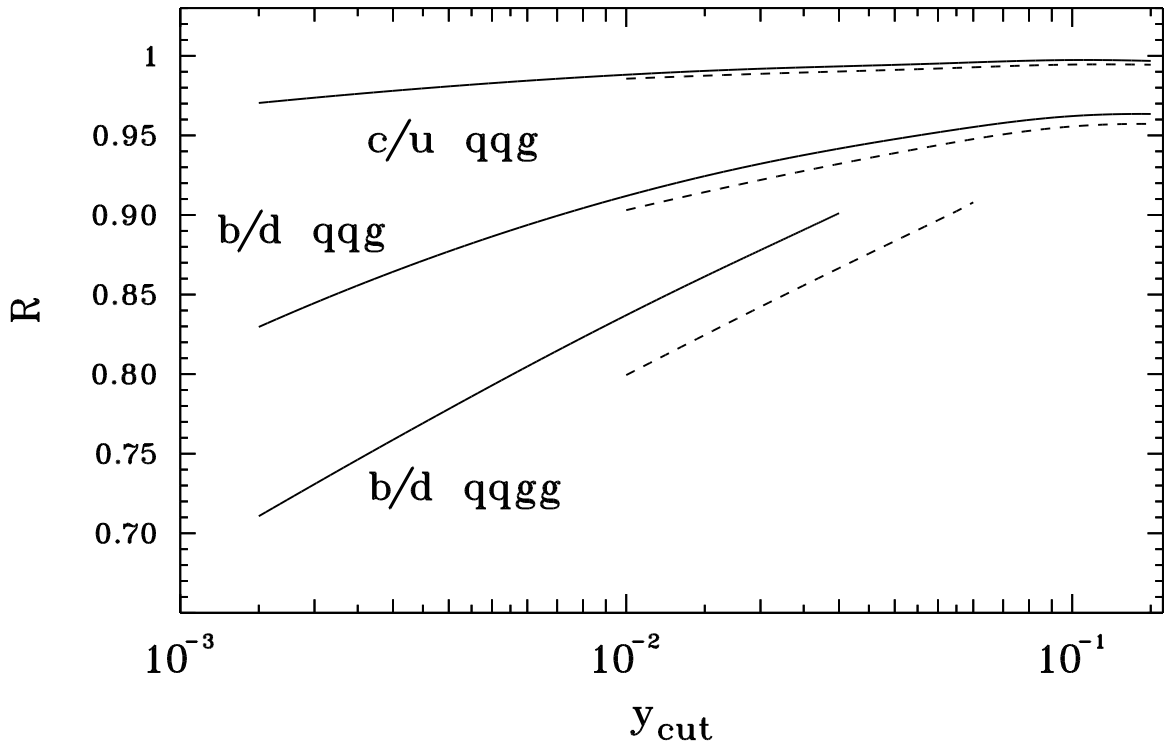
R
1
0.95
0.90
0.85
0.80
0.75
0.70
c/u qqg
b/d qqg
b/d qqgg
10^{-3}
10^{-2}
10^{-1}
y_{cut}

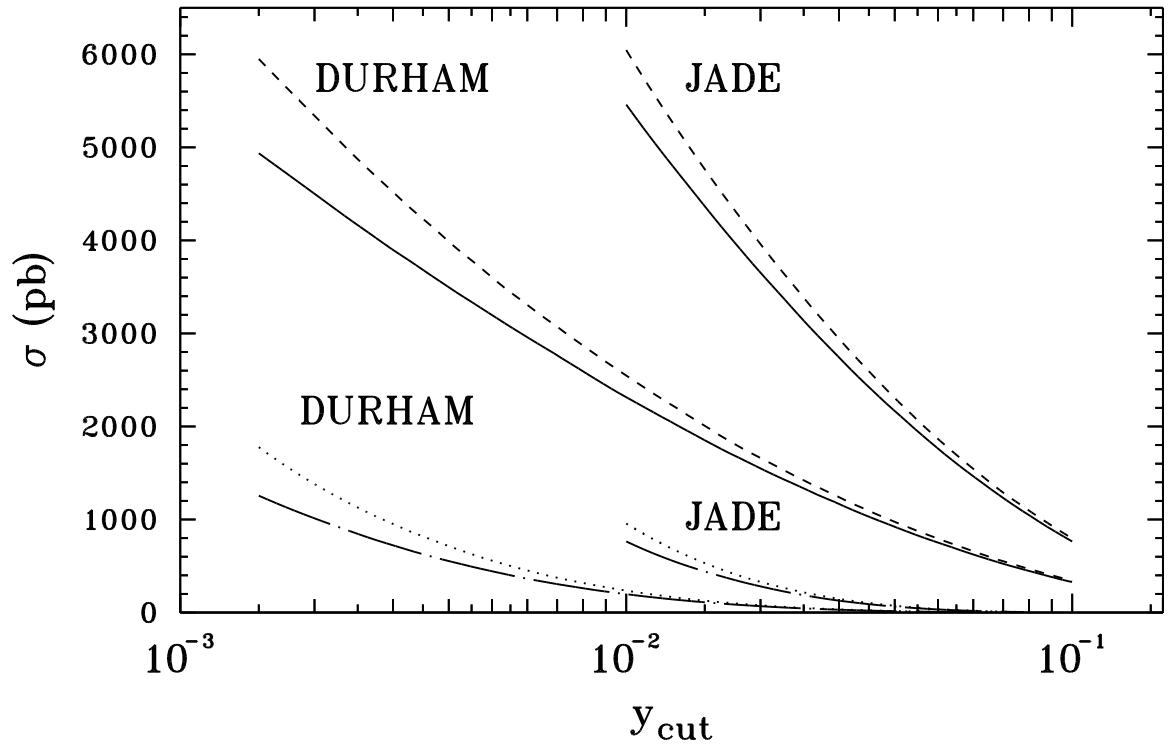
σ (pb)
6000
5000
4000
3000
2000
1000
0
DURHAM
JADE
DURHAM
JADE
10^{-3}
10^{-2}
10^{-1}
y_{cut}

Fig. 1

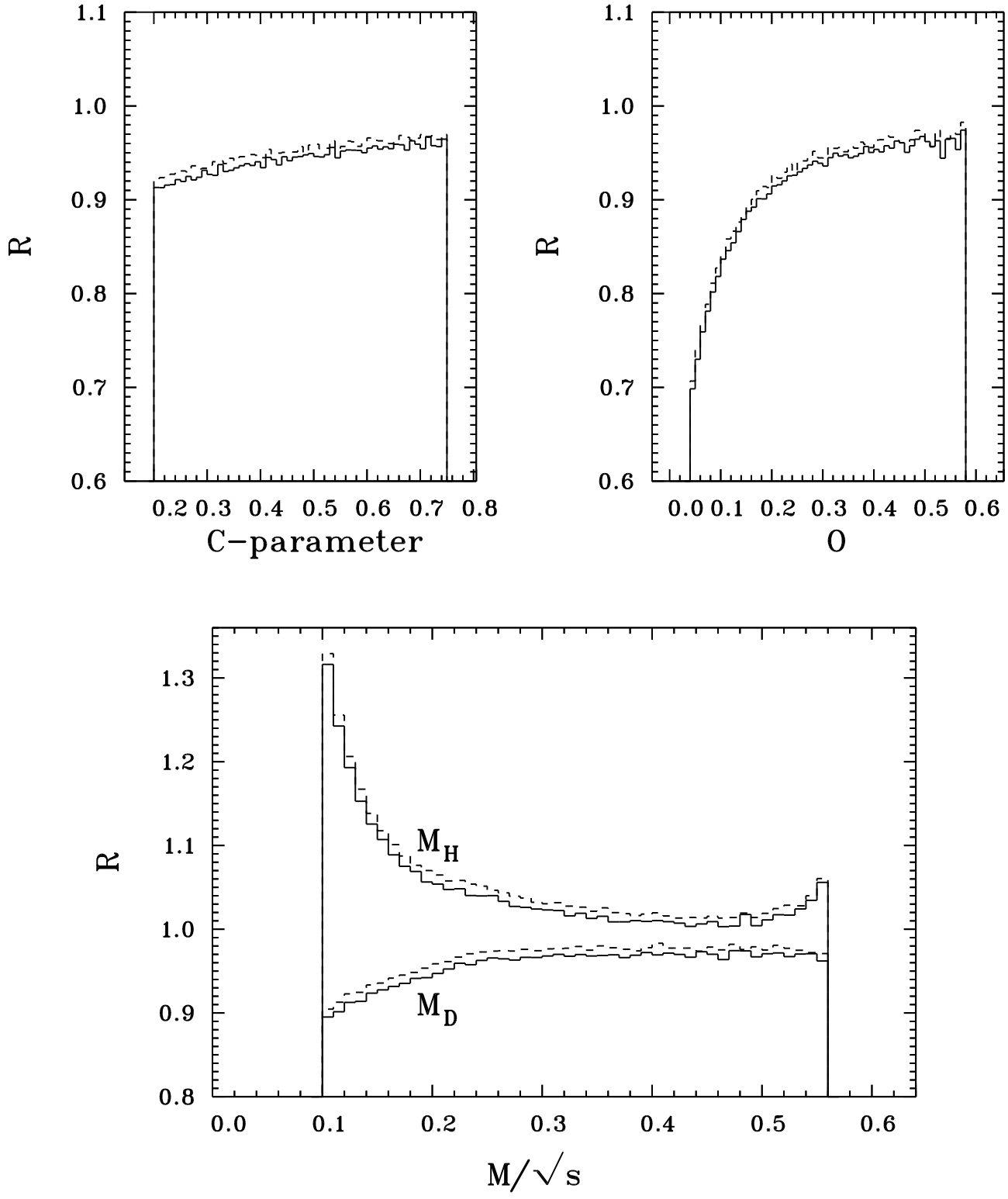

Fig. 2

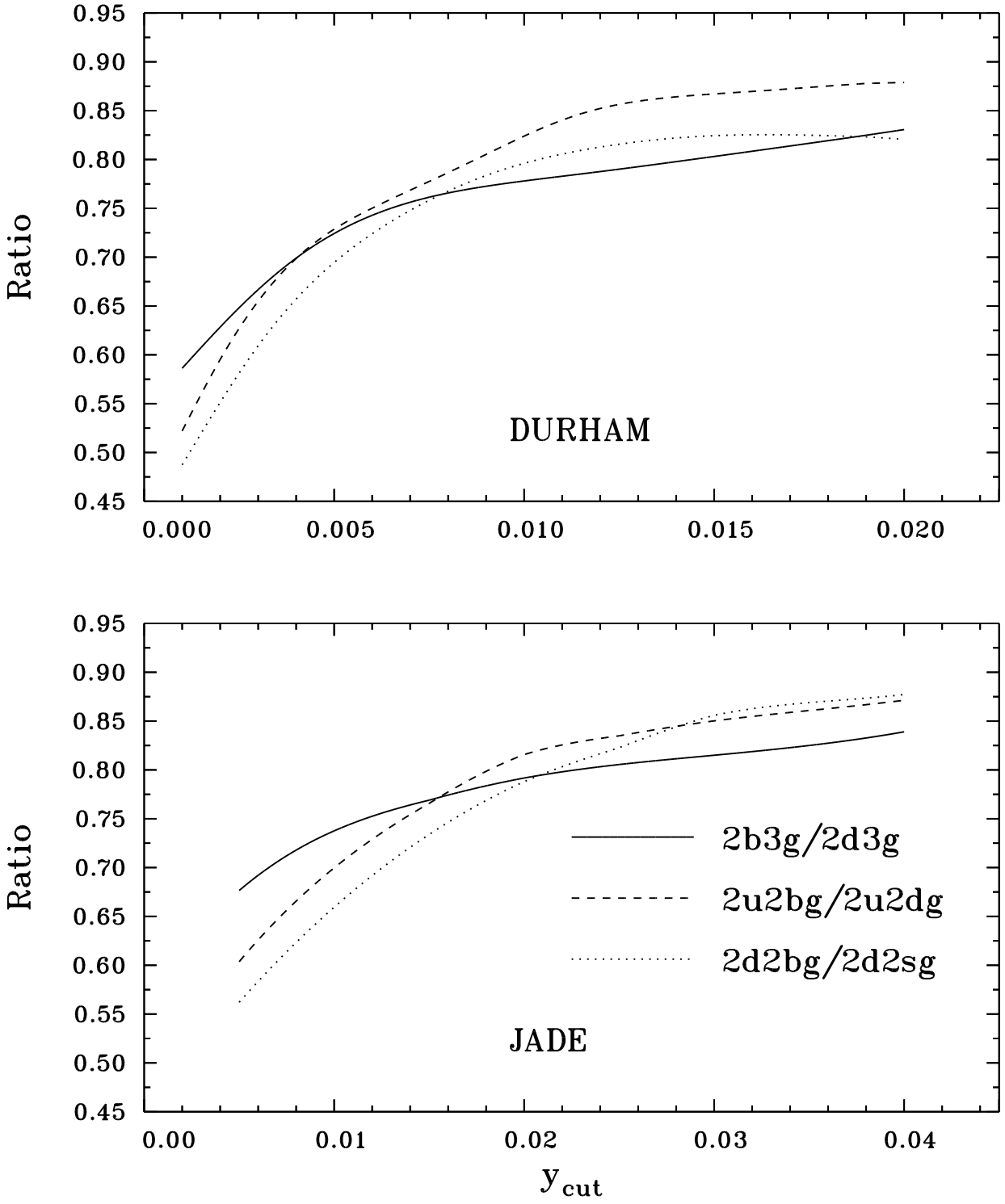
Ratio
0.95
0.90
0.85
0.80
0.75
0.70
0.65
0.60
0.55
0.50
0.45
0.000
0.005
0.010
0.015
0.020
DURHAM
Ratio
0.95
0.90
0.85
0.80
0.75
0.70
0.65
0.60
0.55
0.50
0.45
0.00
0.01
0.02
0.03
0.04
y_{cut}
2b3g/2d3g
2u2bg/2u2dg
2d2bg/2d2sg
JADE

Fig.3